frontiers in Chemistry

ORIGINAL RESEARCH
published: 12 November 2020
doi: 10.3389/fchem.2020.594039

Apolar Polyisoprenoids Located in the Midplane of the Bilayer Regulate the Response of an Archaeal-Like Membrane to High Temperature and Pressure

Josephine G. LoRicco[1], Marta Salvador-Castell[1†], Bruno Demé[2], Judith Peters[2,3] and Philippe M. Oger[1]**

[1] Univ Lyon, INSA de Lyon, CNRS, MAP UMR 5240, Villeurbanne, France, [2] Department of Large Scale Structures, Institut Laue-Langevin, Grenoble, France, [3] Department of Spectroscopy, Université Grenoble Alpes, LiPhy, Grenoble, France

OPEN ACCESS

Edited by:
Olaf Holderer,
Helmholtz Association of German Research Centers (HZ), Germany

Reviewed by:
Arkaprabha Konar,
Kent State University, United States
Maikel Rheinstadter,
McMaster University, Canada

***Correspondence:**
Judith Peters
jpeters@ill.fr
Philippe M. Oger
philippe.oger@insa-lyon.fr

†Present address:
Marta Salvador-Castell,
University of California, San Diego,
La Jolla, CA, United States

Specialty section:
This article was submitted to Physical Chemistry and Chemical Physics,
a section of the journal Frontiers in Chemistry

Received: 12 August 2020
Accepted: 13 October 2020
Published: 12 November 2020

Citation:
LoRicco JG, Salvador-Castell M, Demé B, Peters J and Oger PM (2020) Apolar Polyisoprenoids Located in the Midplane of the Bilayer Regulate the Response of an Archaeal-Like Membrane to High Temperature and Pressure. Front. Chem. 8:594039. doi: 10.3389/fchem.2020.594039

Archaea are known to inhabit some of the most extreme environments on Earth. The ability of archaea possessing membrane bilayers to adapt to high temperature (>85°C) and high pressure (>1,000 bar) environments is proposed to be due to the presence of apolar polyisoprenoids at the midplane of the bilayer. In this work, we study the response of this novel membrane architecture to both high temperature and high hydrostatic pressure using neutron diffraction. A mixture of two diether, phytanyl chain lipids (DoPhPC and DoPhPE) and squalane was used to model this novel architecture. Diffraction data indicate that at high temperatures a stable coexistence of fluid lamellar phases exists within the membrane and that stable coexistence of these phases is also possible at high pressure. Increasing the amount of squalane in the membrane regulates the phase separation with respect to both temperature and pressure, and also leads to an increase in the lamellar repeat spacing. The ability of squalane to regulate the ultrastructure of an archaea-like membrane at high pressure and temperature supports the hypothesis that archaea can use apolar lipids as an adaptive mechanism to extreme conditions.

Keywords: archaea, archaeal lipids, high pressure, phase coexistence, membrane architecture, adaptation, membrane

INTRODUCTION

According to the Singer-Nicolson model, cell membranes are composed of a "mosaic" of proteins embedded in a fluid, lipid bilayer (Singer and Nicolson, 1972). Our understanding of cell membranes has developed further since then, for example we now recognize the importance of other lipid phases in addition to the fluid lamellar phase (bilayer phase), and that there can be substantial lateral heterogeneity within the membrane (Goñi, 2014). Membrane structural lipids, typically phospholipids, are diverse and display varied properties owing to the differences in both the lipid polar head groups and the hydrophobic tails. In aqueous solution, these lipids, driven by the hydrophobic effect, self-assemble into structures in which the hydrophilic heads can interact with the solution and the hydrophobic tails are excluded. The most biologically common phases, seen in familiar lipid bilayer structures, are lamellar phases in which the lipids assemble into flat

sheets (zero membrane curvature) (Cullis et al., 1991; Perutková et al., 2009; Frolov et al., 2011; Goñi, 2014). However, the ability of membrane to form phases with non-zero curvature, such as cubic or inverted hexagonal phases, is also important and plays a role in many cellular processes such as membrane fission and fusion (Jouhet, 2013; McMahon and Boucrot, 2015; Jarsch et al., 2016). Membrane lipids can prefer different membrane curvatures based on their shape, and this preferred curvature can vary with environmental conditions such as pressure and temperature. The presence of diverse lipids within a membrane can even promote phase separation and domain formation within the membrane (Jouhet, 2013). Domains are laterally organized membrane regions with distinct lipid compositions and specialized functions such as interacting with specific proteins, or adopting a specific curvature (Tayebi et al., 2012; Arumugam and Bassereau, 2015; Marquardt et al., 2015). Such lateral membrane domains have been well-characterized in eukaryotic and bacterial cells (Baumgart et al., 2003; Heberle and Feigenson, 2011; Heberle et al., 2013; McCarthy et al., 2015; Schmid, 2017).

Life has been found at some of the most extreme conditions on Earth such as temperatures above 100°C and pressures up to 120 MPa (Yayanos et al., 1981; Takai et al., 2008; Zeng et al., 2009; Dalmasso et al., 2016; Siliakus et al., 2017). All aspects of these organisms must be specially adapted to tolerate such conditions. Cell membranes, in particular, are highly sensitive to pressure and temperature (Winter and Jeworrek, 2009; Oger and Jebbar, 2010; Brooks and Seddon, 2014). In order to maintain functionality of the membrane under extreme conditions cells adjust the composition of their membranes to cope with environmental changes, in a process known as homeoviscous adaptation (Sinensky, 1974). High temperature tends to increase membrane fluidity, permeability, and promote more negative membrane curvature whereas increasing pressure tends to have the opposite effects (Brooks, 2014). To compensate, bacteria and eukaryotes are known to regulate the length, saturation, and branching of the hydrophobic chains as well as the proportion of different polar headgroups (Jebbar et al., 2015; Siliakus et al., 2017). In archaea the mechanisms of adaptation are less well-understood, in part due to their unique membrane lipids. Archaeal lipids have methyl-branched phytanyl chains rather than straight chain fatty acids which are linked via ether rather than ester bonds to the glycerol backbone (De Rosa et al., 1986; Gambacorta et al., 1995). These lipids have higher temperature stability, and lowered proton permeability (Gliozzi et al., 1983; Yamauchi et al., 1993) compared with typical bacterial/eukaryotic lipids.

In addition to bilayer forming lipids, archaea are known to produce bipolar, tetra-ether lipids capable of forming lipid monolayers with high stability and low permeability (De Rosa et al., 1983; Elferink et al., 1994). Archaea have been shown to increase the quantity of tetra-ether lipids in the membrane in response to temperature (Matsuno et al., 2009; Cario et al., 2015). Even some bacteria have shown to produce membrane spanning tetraether or tetraester lipids in response to high-temperature conditions (Damsté et al., 2007; Schouten et al., 2007; Siliakus et al., 2017). Despite the link to high temperature adaption, tetra-ether lipids are not found solely in thermophiles but have also been observed in mesophilic archaea. In addition, not all organisms living at high temperatures produce large quantities, if any tetra-ether lipids (Tornabene and Langworthy, 1979; Hafenbradl et al., 1996; Sako et al., 1996; Sprott et al., 1997; Siliakus et al., 2017). Some insight into the ability of archaea with bilayer forming lipids to live at temperatures up to 100°C can be found in the study by Cario et al. (2015) on the piezo-hyperthermophilic archaeon, *Thermococcus barophilus*. The quantity and saturation of isoprenoid derivatives (such as lycopane, squalane) were shown to vary in response to temperature and pressure. In order to explain the ability of *T. barophilus* to live at high temperature in presence of bilayer forming lipids, it was hypothesized that apolar lipids sit at the midplane of the bilayer and provide enhanced stability (Cario et al., 2015). The ability of apolar lipids such as squalane to localize to the midplane of the lipid bilayer has been confirmed in model membranes of both bacterial-like and archaea-like lipids (Hauß et al., 2002; Salvador-Castell et al., 2020b). The presence of apolar molecules is capable of modulating membrane physicochemical properties, for example, the presence of squalane at the bilayer midplane has been shown to increase permeability to water and decrease proton permeability (Haines, 2001). Apolar molecules at the midplane have been shown to increase the tendency toward negative membrane curvature by reducing packing frustration (Salvador-Castell et al., 2020a,b) and to play a role in phase separation and domain formation (Gilmore et al., 2013; Salvador-Castell et al., 2020b). Such isoprenoid hydrocarbons are found in all archaea (Langworthy et al., 1982) suggesting this hypothesis could be extended to explain adaptation to high temperature and pressure in other archaea processing lipid bilayers.

In this work we studied the behavior of an archaeal-like bilayer with the proposed novel architecture composed of 1,2-di-O-phytanyl-*sn*-glycero-3-phosphocholine (DoPhPC) and 1,2-di-O-phytanyl-*sn*-glycero-3-phosphoethanolamine (DoPhPE) and 2,6,10,15,19,23-hexamethyltetracosane (squalane) under high temperature and high pressure conditions, mimicking the extreme conditions in which some archaea live. Using neutron diffraction, we are able to see the localization of squalane in the midplane bilayer, and to detect the presence of coexisting lamellar phases within the membrane. The structure of each phase as well as the phase coexistence were shown to vary in response to temperature and pressure. The response of the membrane ultrastructure to temperature and pressure could be modulated by varying the quantity of the apolar lipid squalane present in the membrane.

MATERIALS AND METHODS

Chemicals

1,2-di-O-phytanyl-*sn*-glycero-3-phosphocholine (DoPhPC) and 1,2-di-O-phytanyl-*sn*-glycero-3-phosphoethanolamine (DoPhPE) were both purchased from Avanti Polar Lipids (Alabaster, USA) in the lyophilized form and utilized without further purification. The isoprenoid used, 2,6,10,15,19,23-hexamethyltetracosane (squalane) was bought from Sigma—Aldrich Co (Montana, USA) in its hydrogenated

form and from CDN Isotopes (Pointe-Claire, Canada), in its deuterated form.

Sample Preparation

Three milligram of DoPhPC:DoPhPE (9:1 molar) and the corresponding amount of either hydrogenated squalane (h-squalane) or deuterated squalane (d-squalane) were dissolved in chloroform:methanol (2:1) and were spread on a silicon wafer using the "rock and roll" method (Tristram-Nagle, 2007) and dried overnight under high vacuum. Next, the sample was hermetically sealed inside an aluminum sample holder containing a 1:1 ratio of H_2O:D_2O (50% D_2O). The sample was left at 50°C for 48 h to allow for complete hydration.

Neutron Diffraction

Neutron diffraction experiments were performed on D16 (Cristiglio et al., 2015) at the Institut Laue-Langevin (Grenoble, France). The incident wavelength was 4.52 Å. The accessible q-range was from 0.06 $Å^{-1}$ to 0.51 $Å^{-1}$. The H_2O/D_2O contrast was 50% D_2O. 50% D_2O was previously found to give both strong diffraction signal and good resolution between the first order peaks of the two lamellar phases. The temperature was carefully controlled by placing the sample holder in a cryostat. Samples were either measured in a high temperature (HT) sample holder or in a HT-high hydrostatic pressure (HHP) cell (Peters et al., 2018). Data obtained at ILL are identified by Salvador-Castell et al. (2019).

Data treatment was performed by LAMP (Richard et al., 1996) and Origin Pro (Version 2019, OriginLab Corperation, Northampton, MA, USA). The integrated intensities of the Bragg peaks were corrected according to the absorption and analyzed by a Gaussian function, as done previously (Salvador-Castell et al., 2020c). The angle (θ) of a Bragg peak is related to the scattering vector (q) by:

$$q = \frac{4\pi \sin(\theta)}{\lambda} \tag{1}$$

where λ is the wavelength. In cases where many orders of diffraction were visible, a linear fit of the form y = a + bx was performed on a plot of peak location (q) vs. diffraction order (h). The slope of the line (Δq) was used to determine the d-spacing using the following equation:

$$d = \frac{2\pi}{\Delta q} \tag{2}$$

In cases where only a single Bragg order was visible, the d-spacing was calculated using the first order peak and corrected based on the y-intercept determined for each sample under conditions where multiple peaks were present.

To locate squalane in the membrane we used the method described in Hauß et al. (2002, 2005) taking advantage of difference scattering density between hydrogen and deuterium. Neutron scattering length density (NSLD) profiles are constructed from the sum of the neutron scattering lengths per unit volume (Marquardt et al., 2015). The NSLD profiles were calculated from a discrete set of Fourier coefficients (F_h) using the following equation (Katsaras, 1995):

$$\rho(z) = \frac{2}{d}\sum_{h=1}^{h_{max}} |F_h|\, v_n \cos\left(\frac{2h\pi}{d} z\right) \tag{3}$$

where d is the lamellar spacing of the bilayer in the z direction, $z \in \left[\frac{-d}{2}, \frac{d}{2}\right]$, $|F_h| = \pm\sqrt{I_h Q_z}$, Q_z is the Lorentz correction factor equal to q for oriented bilayers, I_h is the integrated intensity of the hth Bragg peak and v_n is the phase of the structure factor. The assigned phases of structure factors 1 to 4 (–, +, +, –) were based on those previously determined for this [DoPhPC:DoPhPE(9:1) + squalane] (Salvador-Castell et al., 2020a).

RESULTS AND DISCUSSION

Stable Phases Coexist Within Archaeal-Like Membrane at High Temperature and Pressure

Cario et al. (2015) proposed a novel membrane architecture to explain the stability of archaea lipid bilayers under high pressure and temperatures. In this novel membrane architecture, apolar lipids act as structural lipids, sitting at the midplane of the lipid bilayer and leading to enhanced membrane stability under extreme conditions (Oger and Cario, 2013; Cario et al., 2015; Salvador-Castell et al., 2020a). A synthetic archaeal-like membrane composed of a mixture of diphytanyl lipids (DoPhPC and DoPhPE in a 9 to 1 molar ratio) and the apolar lipid squalane was used to model this novel architecture. The chemical structures of these lipids are shown in **Supplementary Figure 1**. In order to probe how this membrane behaves under the extreme conditions of temperature and pressure faced by archaea, neutron diffraction was performed on oriented stacked bilayers at temperatures up to 85°C and pressures up to 1,000 bar. Experiments were performed with both hydrogenated squalane (h-squalane) and deuterated squalane (d-squalane) in order to take advantage of the differential neutron scattering between hydrogen and deuterium (Hauß et al., 2002, 2005). The neutron scattering length density (NSLD) for membranes containing h-squalane and d-squalane was plotted as a function of distance (**Supplementary Figure 2**). For convenience, 0 Å represents the midplane of the bilayer. These plots exhibit two characteristic maxima corresponding to the glycerol backbone and a minimal intensity near the terminal methyl groups. The spectra for the membrane containing h-squalane and d-squalane overlap fairly well except within the region corresponding to the midplane of the bilayer (−10 to 10 Å) where the sample containing d-squalane shows an excess of scattering density. This indicates that squalane is located in the midplane of the bilayer and is in agreement with the findings of Salvador-Castell et al. (2020b). In this work we see that this localization of squalane is seen in both $Phase_{LT}$ and $Phase_{HT}$ at low (20 bar) and high (1,000 bar) pressure.

The stacked multilayers were sufficiently ordered in the membrane to give rise to Bragg peaks in the diffraction data. **Figure 1A** shows the 1D neutron diffraction profiles for a membrane composed of DoPhPC:DoPhPE (9:1) + 5 mol% h-squalane at 20 bar (black spectra). The temperature increased

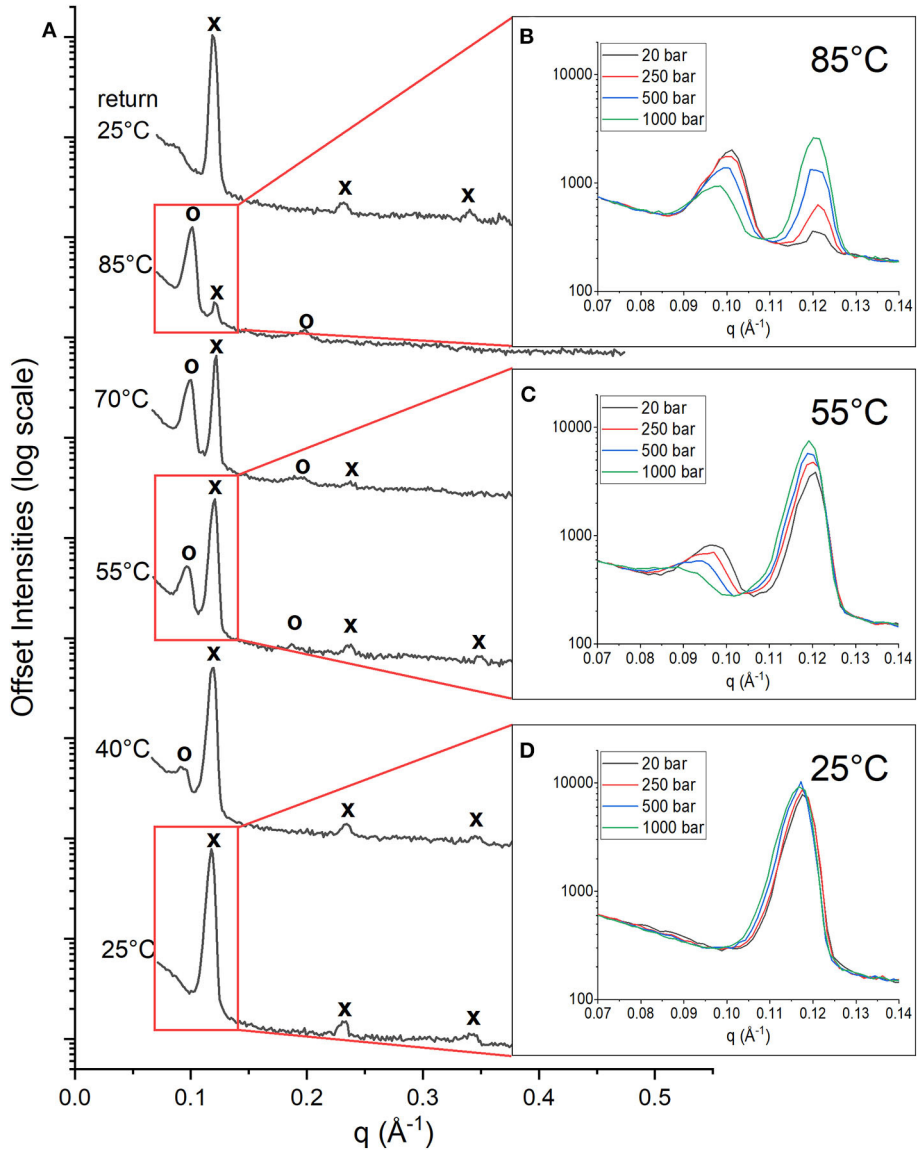

FIGURE 1 | 1D Neutron diffractograms of DoPhPC:DoPhPE (9:1) + 5 mol% h-squalane membrane. **(A)** Diffractograms at 20 bar and temperatures increasing from 25 to 85°C and after returning to 25°C. Diffraction peaks corresponding to $Phase_{LT}$ are denoted with an "x" and peaks corresponding to $Phase_{HT}$ are denoted with an "o." First order diffraction peaks at 85°C **(B)**, 55°C **(C)**, and 25°C **(D)** measured at 20 bar (black), 250 bar (red), 500 bar (blue), and 1,000 bar (green).

from 25°C (bottom) to 85°C (top). At 25°C, there were three orders of diffraction for the sample at low pressure (20 bar). The first order diffraction peak was located at q = ∼0.12 $Å^{-1}$, the second order peak at q = ∼0.23 $Å^{-1}$, and the third order peak at q = ∼0.34 $Å^{-1}$. The location of peaks in the ratio of (1, 2, 3...) indicates a lamellar phase (Tyler et al., 2015). As the temperature increased, the peaks corresponding to the original phase were still present at similar values of q (marked with an "x"), although with diminished intensities. At higher temperatures (above 40°C) a second set of peaks appeared at lower values of q corresponding to a new phase (marked with an "o"). The first order diffraction peak of this new phase is located at q = ∼0.09 $Å^{-1}$ and the second order diffraction peak at q = ∼0.18 $Å^{-1}$. The spacing of the peaks indicates that this new phase is also lamellar. We will refer to the new phase as $Phase_{HT}$ because it appeared at high temperatures (HT) compared to the original phase, which is also present at low temperatures (LT) and will therefore be referred to as $Phase_{LT}$. Increasing temperature leads to an increase in the intensity of the $Phase_{HT}$ peaks indicating that temperature stabilizes $Phase_{HT}$, and leads to a decrease in the intensity of $Phase_{LT}$ indicating that temperature destabilizes $Phase_{LT}$. Upon returning the membrane to 25°C and 20 bar, the initial state, is restored indicating that this change in phase is fully reversible (**Figure 1A**).

At each temperature, the diffraction of the DoPhPC:DoPhPE (9:1) + 5 mol% h-squalane membrane was measured at 20, 250, 500, and 1,000 bar. The **Figure 1** insets show the first order

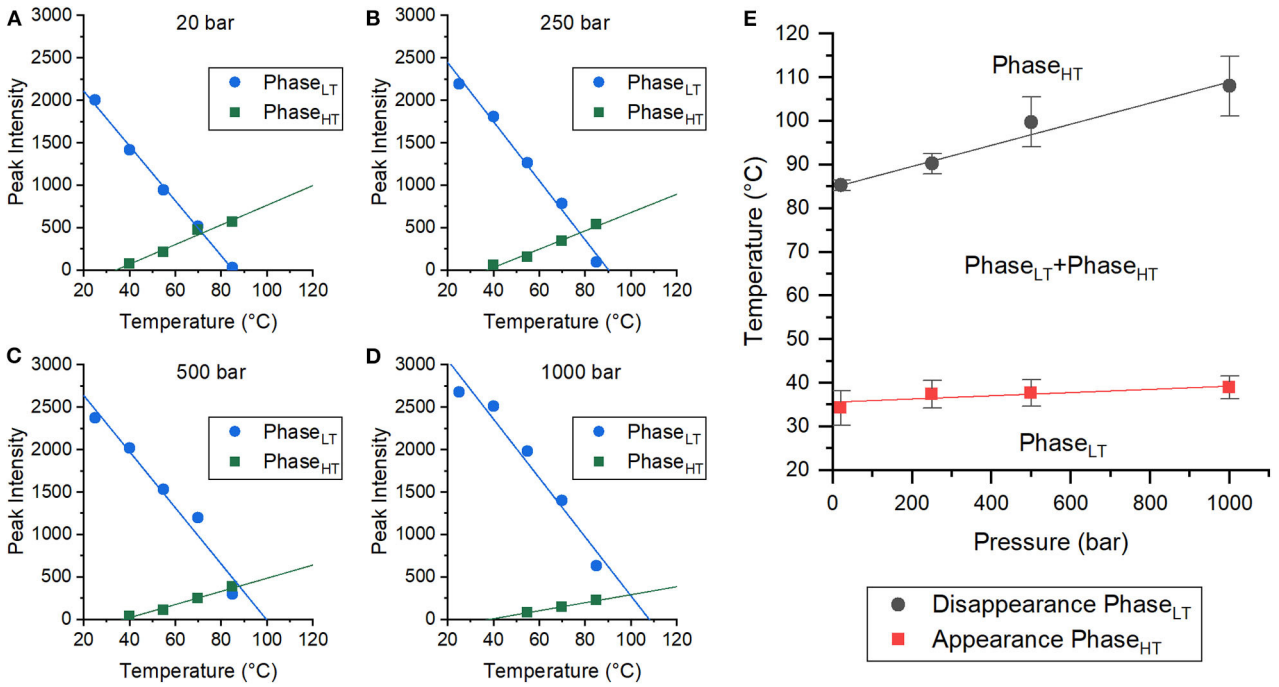

FIGURE 2 | Coexistence of phases in DoPhPC:DoPhPE (9:1) membrane containing 5 mol% h-squalane. **(A–D)** Plots of peak intensities of Phase$_{LT}$ (blue circles) and Phase$_{HT}$ (green squares) as a function of temperature. Pressures were 20 bar **(A)**, 250 bar **(B)**, 500 bar **(C)**, and 1,000 bar **(D)**. Error bars are within symbols. **(E)** Pressure-Temperature diagram of the coexistence of Phase$_{LT}$ and Phase$_{HT}$. Error bars indicate standard errors.

diffraction peaks, indicated by the red boxes, seen at pressures of 20 bar (black), 250 bar (red), 500 bar (blue) and 1,000 bar (green). At 85 and 55°C, two first order diffraction peaks are seen, representing the two phases. The area of the Phase$_{HT}$ peak (found at lower q) decreases and the area of the Phase$_{LT}$ peak (found at higher q) increases as a function of pressure (**Figures 1B,C**). This indicates that high pressure has a stabilizing effect on Phase$_{LT}$ and a destabilizing effect on Phase$_{HT}$. Although it is well-established that increasing pressure causes an effect similar to decreasing the temperature, our results show that even 1,000 bar is not enough to completely replace Phase$_{HT}$ and return to the lipid organization present at lower temperatures. At 25°C, the membrane is exclusively in Phase$_{LT}$. Again, there is a slight increase in the intensity of the Phase$_{LT}$ peak with pressure indicating that pressure stabilizes Phase$_{LT}$ (**Figure 1D**).

Both pressure and temperature play an important role in the stability of each phase and their ability to coexist. In order to better quantify the temperature and pressure range at which these phases coexist, the change in the integrated peak intensities was monitored as a function of temperature at each pressure (20, 250, 500, and 1,000 bar). The changes in the peak intensities of the first order peaks of both Phase$_{LT}$ and Phase$_{HT}$ have a linear dependence on temperature (**Figures 2A–D**, **Supplementary Figure 3**). A linear fit could be used to extrapolate/interpolate when the peak intensity would be zero and thus to determine the temperature at which the corresponding phase was no longer present in the membrane for each pressure, as shown in **Figure 2**.

The integrated peak intensities of Phase$_{LT}$ (blue) and Phase$_{HT}$ (green) at 20 bar were analyzed as a function of temperature (**Figure 2A**). A linear fit of the integrated Phase$_{HT}$ peak intensities determined that the peak intensity would equal zero at 34.3 ± 3.9°C, signifying that Phase$_{HT}$ appears above this temperature. Below this temperature, the membrane is exclusively in Phase$_{LT}$. A linear fit of the Phase$_{LT}$ peak intensities determined that the peak intensity would reach zero at 85.3 ± 1.2°C. Above this temperature, Phase$_{LT}$ would disappear and the membrane would be entirely in Phase$_{HT}$. Between these two temperatures, both phases coexist. This analysis was repeated with the data taken at 250, 500, and 1,000 bar (**Figures 2B–D**), allowing the determination of a pressure-temperature diagram of the phase coexistence of Phase$_{LT}$ and Phase$_{HT}$ (**Figure 2E**). The temperature at which Phase$_{HT}$ appears (T_{HT}) increased with increasing pressure from 34.3 ± 3.9°C at 20 bar to 37.4 ± 3.2°C at 250 bar, 37.7 ± 3.0°C at 500 bar, and to 38.9 ± 2.6°C at 1,000 bar. The increase in T_{HT} with pressure was small (∼5°C/kbar) and was not statistically significant. The temperature at which Phase$_{LT}$ disappeared (T_{LT}) also increased with increasing pressure from 85.3 ± 1.2°C at 20 bar, to 90.2 ± 2.3°C at 250 bar, 99.7 ± 5.7°C at 500 bar, and finally to 108.0 ± 6.9°C at 1,000 bar. The increase in T_{LT} as a function of pressure was much larger (∼24°C/kbar) (**Figure 2E**). Here we demonstrate that although the phases are pressure sensitive, phase coexistence is possible at pressures up to, and presumably above, 1,000 bar. Based on the phase diagram, at high temperatures (> 85°C), the application of pressure

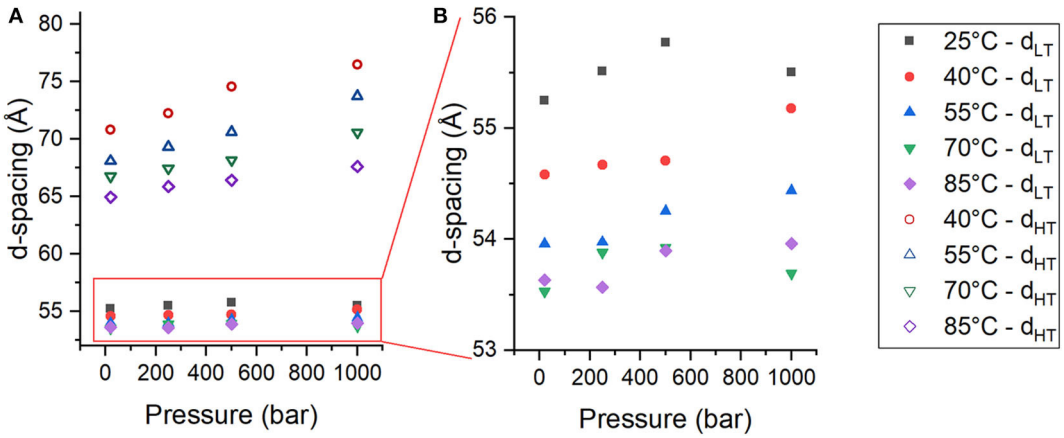

FIGURE 3 | (A,B) Membrane d-spacing as a function of pressure for $Phase_{LT}$ (solid symbols) and $Phase_{HT}$ (open symbols) in DoPhPC:DoPhPE (9:1) membrane containing 5 mol% h-squalane. Temperature was 25°C (black squares), 40°C (red circles), 55°C (blue triangles), 70°C (green inverted triangles), or 85°C (purple diamonds). Error for d-spacing measurements is ± 0.5 Å.

is predicted to induce phase separation from solely $Phase_{HT}$ at low pressure to a coexistence of $Phase_{HT}$ and $Phase_{LT}$ at high pressure and high temperature. Pressure induced phase separation is not a novel concept, as high pressure has been previously shown to be capable of inducing phase separation and domain formation (McCarthy et al., 2015). Our results suggest that this is also possible in membranes composed of archaeal lipids. It should be noted that the T_{HT} and T_{LT} reported here were calculated only as the sample being heated, and that the transition temperature upon cooling was not explicitly tracked. Membranes are known to exhibit hysteresis near phase transitions meaning that the transition temperatures upon heating and cooling are different. A similar effect has also been seen in membranes upon pressurization/depressurization (Trovaslet-Leroy et al., 2016).

From the changes in peak intensity, it could be determined that pressure destabilizes $Phase_{HT}$ and stabilizes $Phase_{LT}$. In addition to changes in the integrated intensities of the peaks, there were also changes in the location of the peaks with pressure that reflect changes in the lamellar repeat structure. The multilayer organization of the membranes makes it simple to determine the repeat spacing (d), which includes the thickness of the bilayer and its associated water layer (Nagle and Tristram-Nagle, 2000), from the location of the Bragg peaks of each phase. For a lamellar phase, the repeat spacing (d) can be calculated simply by Equation (3), where q is the location of the first order lamellar peak. The d-spacing of both $Phase_{LT}$ (solid symbols) and $Phase_{HT}$ (open symbols) increase as a function of pressure (**Figure 3A**). The d-spacing of $Phase_{LT}$ with increasing pressure is shown again in **Figure 3B** using a different scale to better visualize the changes. $Phase_{LT}$ exhibits either a small increase or negligible change in d-spacing with increasing pressure. Linear fitting of the data determined that the d-spacing of $Phase_{LT}$ increases at a rate of 0.23 ± 0.32 Å/kbar at 25°C, 0.61 ± 0.13 Å/kbar at 40°C, 0.53 ± 0.11 at 55°C, 0.09 ± 0.30 at 70°C and 0.40 ± 0.16 at 85°C. An increase in membrane d-spacing with pressure has been observed previously (Winter and Jeworrek, 2009; Trapp et al., 2013; Brooks and Seddon, 2014). Increasing pressure provokes a lateral compression of membrane lipids and an increase in membrane thickness due to extension of the hydrocarbon chains. The d-spacing of $Phase_{HT}$ also increases with pressure (**Figure 3A**). The d-spacing increased at a rate of 5.84 ± 0.81 Å/kbar at 40°C, 5.78 ± 0.19 Å/kbar at 55°C, 3.91 ± 0.36 Å/kbar at 70°C, and 2.62 ± 0.22 Å/kbar at 85°C. The changes in d-spacing for $Phase_{HT}$ were almost an order of magnitude greater than that seen in $Phase_{LT}$ showing that $Phase_{HT}$ is much more sensitive to changes in pressure. It is interesting to note that the swelling of $Phase_{HT}$ decreases with temperature.

The formation of a new phase, $Phase_{HT}$, is most likely due to the presence of lipids with different preferred curvatures within the membrane as seen by Salvador-Castell et al. (2020b). The bilayer is made up of two phytanyl lipids with different polar head groups (DoPhPC and DoPhPE) and the apolar isoprenoid squalane. The phosphoethanolamine (PE) headgroup is small, so the lipid has a conical geometry and favors a negative curvature (favoring the formation of non-lamellar structure such as inverted hexagonal phases/cubic phases/inverted micelles). The phosphocholine (PC) headgroup is larger and the lipid has a cylindrical geometry which favors zero-curvature (favoring the formation of lamellar structures such as bilayers). The PC headgroup can stabilize the lamellar phase of PE lipids (Kates and Manson, 1984). The phase separation can be explained by partitioning of DoPhPC and DoPhPE into different phases based on preferred curvature which can be triggered, for example, by temperature which favors more negative membrane curvatures. The presence of squalane also promotes negative lipid curvature and was found to forward the formation of non-lamellar phases in a DoPhPC:DoPhPE (9:1) membrane (Salvador-Castell et al., 2020a,b). Increasing pressure, on the other hand, tends to increase the preferred membrane curvature (Shearman et al., 2006; Brooks, 2014). In our model membrane, phase separation was triggered by increasing temperature, which could be due to the differences in curvature between the lipids becoming

TABLE 1 | Membrane d-spacing for $Phase_{LT}$ (left table) and $Phase_{HT}$ (right table) for DoPhPC:DoPhPE (9:1) membrane containing h-squalane.

$Phase_{LT}$	+2.5% squalane	+5% squalane	+10% squalane	$Phase_{HT}$	+2.5% squalane	+5% squalane	+10% squalane
25°C 20 bar	55.6 Å	55.2 Å	56.0 Å	25°C 20 bar	N.P.	N.P.	82.3 Å
25°C 250 bar	56.2 Å	55.5 Å	57.0 Å	25°C 250 bar	N.P.	N.P.	86.7 Å
25°C 500 bar	56.1 Å	55.8 Å	57.1 Å	25°C 500 bar	N.P.	N.P.	88.9 Å
25°C 1,000 bar	56.2 Å	55.5 Å	57.2 Å	25°C 1000bar	N.P.	N.P.	90.6 Å
40°C 20 bar	55.2 Å	54.6 Å	55.7 Å	40°C 20 bar	N.P.	70.8 Å	78.6 Å
40°C 250 bar	55.2 Å	54.7 Å	55.8 Å	40°C 250 bar	N.P.	72.2 Å	79.8 Å
40°C 500 bar	55.0 Å	54.7 Å	56.0 Å	40°C 500 bar	N.P.	74.6 Å	82.6 Å
40°C 1,000 bar	55.6 Å	55.2 Å	56.4 Å	40°C 1,000 bar	N.P.	76.5 Å	83.6 Å
55°C 20 bar	54.1 Å	54.0 Å	55.3 Å	55°C 20 bar	67.1 Å	68.1 Å	74.7 Å
55°C 250 bar	54.8 Å	54.0 Å	55.7 Å	55°C 250 bar	68.5 Å	69.3 Å	75.9 Å
55°C 500 bar	55.2 Å	54.3 Å	55.3 Å	55°C 500 bar	69.4 Å	70.6 Å	77.3 Å
55°C 1,000 bar	55.2 Å	54.4 Å	56.1 Å	55°C 1,000 bar	72.2 Å	73.7 Å	80.0 Å
70°C 20 bar	53.8 Å	53.5 Å	54.4 Å	70°C 20 bar	65.7 Å	66.8 Å	72.4 Å
70°C 250 bar	54.0 Å	53.9 Å	55.3 Å	70°C 250 bar	65.7 Å	67.5 Å	74.3 Å
70°C 500 bar	54.2 Å	53.9 Å	55.2 Å	70°C 500 bar	67.7 Å	68.2 Å	74.1 Å
70°C 1,000 bar	54.8 Å	53.7 Å	55.2 Å	70°C 1,000 bar	70.1 Å	70.6 Å	75.3 Å
85°C 20 bar	53.5 Å	53.6 Å	N.P.	85°C 20 bar	64.9 Å	65.0 Å	74.1 Å
85°C 250 bar	53.5 Å	53.6 Å	54.3 Å	85°C 250 bar	65.4 Å	65.9 Å	75.4 Å
85°C 500 bar	53.6 Å	53.9 Å	54.5 Å	85°C 500 bar	65.9 Å	66.4 Å	74.8 Å
85°C 1,000 bar	53.7 Å	54.0 Å	54.8 Å	85°C 1,000 bar	67.3 Å	67.6 Å	76.3 Å

N.P., not present. Error is ± 0.5 Å.

too great to remain within the same phase. Increasing pressure hinders the phase separation and favors $Phase_{LT}$, lending further support to the idea that the phase separation is driven by components of different curvature.

Increasing negative curvature favors a transition from a lamellar phase to a non-lamellar phase. Although no such phases were seen by neutron diffraction, non-lamellar phases in this membrane system have been detected by SAXS (Salvador-Castell et al., 2020a). Neutron scattering was performed on multi-stacks of bilayers on a silicon wafer, whereas for the SAXS the sample was not ordered on a substrate but rather was self-assembled in bulk. These differences in lipid preparation may explain why in one case the DoPhPC:DoPhPE (9:1) + 5 mol% squalane membrane separates into two lamellar phases and in the other case the membrane separates into a lamellar phase and an inverted hexagonal phase. The ordering of the lipids on a solid support for neutron diffraction may impede the formation of non-lamellar phases. For both phases seen by neutron diffraction, increasing pressure leads to an increase in the membrane d-spacing, however, the magnitude of the pressure-induced swelling was significantly different between the phases. The changes in $Phase_{LT}$ are small, generally within the error of the measurements for the d-spacing. The changes in $Phase_{HT}$ are quite large (2–6 Å/kbar). The pressure-induced swelling of the $Phase_{HT}$ seen by neutron diffraction is unusually large for a lamellar phase which is typically <2 Å/kbar (Brooks, 2014). Interestingly, the magnitude of the pressure-induced swelling seen in $Phase_{HT}$ is similar to that seen in the inverted hexagonal phase seen by SAXS (Salvador-Castell et al., 2020a). **Supplementary Figure 4** illustrates how the membrane lattice parameter (equal to d for lamellar phase and 2/3 d for inverted hexagonal phase) increases as a function of pressure. The similarities in the response to pressure of $Phase_{HT}$ and the inverted hexagonal phase seen in SAXS could be due to the partitioning of lipid headgroups and squalane in a similar manner.

Squalane Regulates Membrane Ultrastructure Under High Temperature and Pressure

Archaea are thought to regulate their membranes response to extreme conditions with apolar lipids. For this reason, the neutron diffraction experiments were repeated with two additional concentrations of hydrogenated squalane, 2.5 and 10 mol% in order to determine what effect the amount of squalane would have on the membrane structure at high temperatures and pressures. Two coexisting phases are also present in membranes containing 2.5 or 10 mol% squalane at elevated temperatures (**Supplementary Figures 5, 6**).

The repeat spacing of $Phase_{LT}$ and $Phase_{HT}$ was calculated for the membranes containing 2.5, 5, and 10 mol% squalane and the values are displayed in **Table 1**. In all membranes, there is an increase in the membrane d-spacing with increasing pressure, and $Phase_{HT}$ is again found to be the more pressure-sensitive phase (**Figure 4**). The pressure induced swelling of $Phase_{LT}$ remains small (≤1Å/kbar) for all squalane concentrations and is not significantly different with changes in temperature. The pressure induced swelling of $Phase_{HT}$ is much larger (2–8 Å/kbar) and the swelling of $Phase_{HT}$ is temperature dependent.

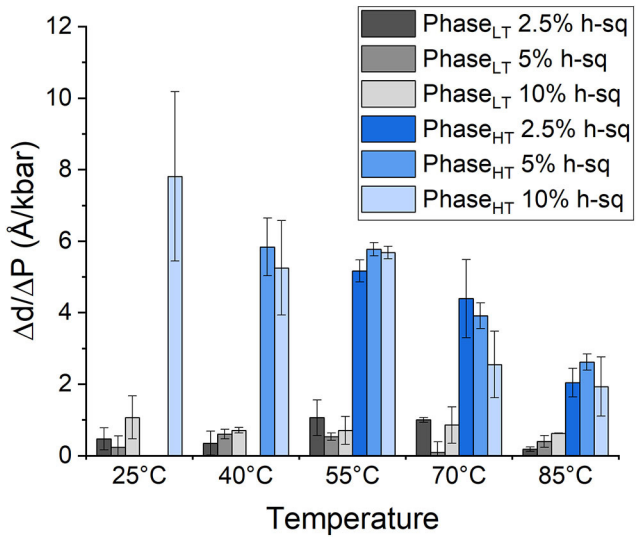

FIGURE 4 | Pressure induced swelling of DoPhPC:DoPhPE (9:1) membrane containing different quantities of h-squalane. Swelling of Phase$_{LT}$ containing 2.5 mol% (dark gray), 5 mol% (gray), or 10 mol% (light gray) h-squalane. Swelling of Phase$_{HT}$ containing 2.5 mol% (dark blue), 5 mol% (blue), or 10 mol% (light blue) h-squalane.

TABLE 2 | Temperature at which Phase$_{HT}$ appears in DoPhPC:DoPhPE (9:1) membrane containing h-squalane.

Pressure	2.5% squalane	5% squalane	10% squalane
20 bar	44.7 ± 4.0°C	34.3 ± 3.9°C	23.9 ± 3.4°C
250 bar	49.3 ± 1.5°C	37.4 ± 3.2°C	28.8 ± 3.3°C
500 bar	49.2 ± 0.1°C	37.7 ± 3.0°C	31.8 ± 1.6°C
1,000 bar	50.8 ± 1.2°C	38.9 ± 2.6°C	32.2 ± 2.6°C

The swelling is significantly larger at low temperatures and smaller at high temperatures. Although the percentage of squalane does not change the swelling of Phase$_{HT}$, the amount of squalane does play an important role in affecting the temperature range at which Phase$_{HT}$ is present. At ≥55°C, Phase$_{HT}$ is seen in membranes containing 2.5, 5, and 10 mol% squalane. At 40°C, Phase$_{HT}$ is no longer capable of forming the membrane containing 2.5 mol% squalane and at 25°C, Phase$_{HT}$ is only seen in the membrane containing 10 mol% squalane.

The temperatures at which Phase$_{HT}$ appears for a membrane containing either 2.5 or 10 mol% squalane are determined from a linear fit of integrated peak intensity vs. temperature (**Supplementary Figure 3**). As seen previously with the membrane containing 5 mol% squalane, pressure leads to an increase in T_{HT} and T_{LT} (**Supplementary Figure 7**). Increasing the quantity of squalane promotes the formation of Phase$_{HT}$ at lower temperatures. For example, at 20 bar Phase$_{HT}$ appears at 44.7 ± 4.0°C for the membrane containing 2.5 mol% squalane, 34.3 ± 3.9°C for the membrane containing 5 mol% squalane and 23.9 ± 3.4°C for the membrane containing 10 mol% squalane. The concentration of squalane has a similar effect on T_{HT} at elevated pressures (**Table 2**).

This agrees with previous findings that squalane promotes negative membrane curvature, favoring the formation of Phase$_{HT}$ and phase separation at lower temperatures (Salvador-Castell et al., 2020a,b). Here we show that squalane is also capable of promoting the formation of Phase$_{HT}$ at high pressures. Previously at ambient pressure, it was shown that the phase coexistence and lateral organization within a DoPhPC:DoPhPE membrane was squalane dependent leading to the hypothesis that squalane may promote the formation of membrane domains (Salvador-Castell et al., 2020b). That would mean that the ability of squalane to favor phase separation at high pressures, may indicate that squalane could also promote domain formation in archaea that live at such high-pressure conditions.

In addition to regulating the phase coexistence within the membrane, increasing the amount of squalane in the membrane also affects the d-spacing. The d-spacing of the membrane is typically higher when the membrane contains a higher quantity of squalane for Phase$_{HT}$ (**Table 1**, **Supplementary Figure 8**). For example, in Phase$_{HT}$ at 20 bar/55°C the d-spacing is 67.1 Å when the membrane contains 2.5 mol% squalane compared with 68.1 Å when the membrane contains 5 mol% squalane and 74.7 Å when the membrane contains 10 mol% squalane. In this experiment, we did not see a significant change in the d-spacing of Phase$_{LT}$ with increasing squalane concentration which was seen previously, at ambient pressure and temperature (Salvador-Castell et al., 2020b). The increase in d-spacing with increasing squalane for Phase$_{LT}$ was only seen up to 5 mol% squalane at which point the phase is thought to reach saturation. It is conceivable that the amount of squalane required to reach saturation within membrane could change with pressure and temperature and this may be one of the reason we did not see any change in the d-spacing of Phase$_{LT}$ with increasing squalane in this experiment.

At temperatures at which Phase$_{HT}$ was present, Phase$_{HT}$ was always found to increase in d-spacing with increasing squalane. Previously it was shown that increasing the percentage of squalane leads to an increase in the d-spacing in Phase$_{LT}$ due to an increase in the hydrophobic core thickness (Salvador-Castell et al., 2020b). The localization of squalane to the midplane of the bilayer is confirmed for Phase$_{HT}$ as well as Phase$_{LT}$ (**Supplementary Figure 2**). This could indicate that the increase in the d-spacing for Phase$_{HT}$ is also due to an increase in hydrophobic core thickness although this cannot be directly confirmed from this data. Increasing squalane promotes changes in membrane structure of both phases, even at high pressures and temperatures, indicating that squalane could act as a membrane regulator under the extreme conditions at which many archaea live.

CONCLUSIONS

It was proposed by Cario et al. (2015) that apolar lipids, such as squalane, sit at the midplane of the lipid bilayer, and provide a means of enhancing the stability of archaeal membrane bilayers under extreme conditions. This localization of apolar lipids to the midplane of an archaeal-like bilayer was then confirmed by the work of Salvador-Castell et al. (2020b). The aims of this

study were to determine how an archaeal-like membrane with this novel membrane architecture behaves in response to the high temperatures and high hydrostatic pressures and to determine how the quantity of apolar lipid present in the membrane modulates this behavior. To model the proposed membrane architecture in which apolar molecules sit in the midplane of the bilayer, we used an artificial archaea-like membrane composed of DoPhPC, DoPhPE, and squalane. The use of neutron diffraction allowed us to confirm the localization of the apolar lipid squalane and to further study the coexistence of two distinct lamellar phases previously reported by Salvador-Castell et al. (2020b). The phase separation within the membrane is most likely due to the partitioning of lipids (DoPhPC/DoPhPE) with different preferred curvatures and the presence of the apolar molecule (squalane). The two phases are capable of coexisting at a wide range of temperatures and pressure. High temperature favors the formation of a swollen lamellar phase ($Phase_{HT}$) and high pressure favors a thinner lamellar phase ($Phase_{LT}$). The temperature and pressure range of the phase coexistence is regulated by the percentage of squalane present in the membrane. Increasing the percentage of squalane favors the formation of $Phase_{HT}$ at lower temperatures, for pressures up to 1,000 bar. Coexistence and lateral organization of these phases was seen previously at ambient pressure (Salvador-Castell et al., 2020b). Here we have shown that phase coexistence is also seen at high pressure which could indicate the possibility of domain formation in archaea living at high pressure in addition to high temperature. Increasing the amount of squalane also leads to an increase in the membrane lamellar repeat spacing for $Phase_{HT}$. The ability of squalane to modify the membrane ultrastructure at both high pressure and temperature supports the hypothesis that apolar lipids play a role in adaptation of archaea to extreme conditions.

DATA AVAILABILITY STATEMENT

The datasets generated for this study can be found in online repositories. The names of the repository/repositories and accession number(s) can be found at: http://dx.doi.org/10.5291/ILL-DATA.8-02-852.

AUTHOR CONTRIBUTIONS

PO, MS-C, and JP conceived the project. MS-C, BD, JP, and PO carried out the experiments. JL performed the data analysis and wrote the initial draft. All authors contributed to the final manuscript.

FUNDING

This work was supported by the French National Research Agency programme ANR 17-CE11-0012-01 to PO and JP. MS-C was supported by a Ph.D. grant from the French Ministry of Research.

ACKNOWLEDGMENTS

The authors thank the Institut Laue-Langevin for the allocation of beamtime (Salvador-Castell et al., 2019) and for technical support with the high temperature and pressure setup.

SUPPLEMENTARY MATERIAL

The Supplementary Material for this article can be found online at: https://www.frontiersin.org/articles/10.3389/fchem.2020.594039/full#supplementary-material

REFERENCES

Arumugam, S., and Bassereau, P. (2015). Membrane nanodomains: contribution of curvature and interaction with proteins and cytoskeleton. *Essays Biochem*. 57, 109–119. doi: 10.1042/bse0570109

Baumgart, T., Hess, S. T., and Webb, W. W. (2003). Imaging coexisting fluid domains in biomembrane models coupling curvature and line tension. *Nature* 425, 821–824. doi: 10.1038/nature02013

Brooks, N. J. (2014). Pressure effects on lipids and bio-membrane assemblies. *IUCrJ* 1, 470–477. doi: 10.1107/S2052252514019551

Brooks, N. J., and Seddon, J. M. (2014). High pressure x-ray studies of lipid membranes and lipid phase transitions. *Zeitschr. Phys. Chem.* 228, 987–1004. doi: 10.1515/zpch-2014-0602

Cario, A., Grossi, V., Schaeffer, P., and Oger, P. M. (2015). Membrane homeoviscous adaptation in the piezo-hyperthermophilic archaeon *Thermococcus barophilus*. *Front. Microbiol.* 6:1152. doi: 10.3389/fmicb.2015.01152

Cristiglio, V., Giroud, B., Didier, L., and Demé, B. (2015). D16 is back to business: more neutrons, more space, more fun. *Neutron News* 26, 22–24. doi: 10.1080/10448632.2015.1057051

Cullis, P. R., Tilcock, C. P., and Hope, M. J. (1991). "Lipid polymorphism," in *Membrane Fusion*, eds J. Wilschut and D. Hoekstra (New York, NY: CRC Press), 35–64.

Dalmasso, C., Oger, P., Courtine, D., Georges, M., Takai, K., Maignien, L., et al. (2016). Complete genome sequence of the hyperthermophilic and piezophilic archeon *Thermococcus piezophilus* CDGST, able to grow under extreme hydrostatic pressures. *Genome Announc.* 4:e00610-16. doi: 10.1128/genomeA.00610-16

Damsté, J. S. S., Rijpstra, W. I. C., Hopmans, E. C., Schouten, S., Balk, M., and Stams, A. J. M. (2007). Structural characterization of diabolic acid-based tetraester, tetraether and mixed ether/ester, membrane-spanning lipids of bacteria from the order thermotogales. *Arch. Microbiol.* 188, 629–641. doi: 10.1007/s00203-007-0284-z

De Rosa, M., Gambacorta, A., and Gliozzi, A. (1986). Structure, biosynthesis, and physicochemical properties of archaebacterial lipids. *Microbiol. Rev.* 50, 70–80. doi: 10.1128/MMBR.50.1.70-80.1986

De Rosa, M., Gambacorta, A., and Nicolaus, B. (1983). A new type of cell membrane, in thermophilic archaebacteria, based on bipolar ether lipids. *J. Memb. Sci.* 16, 287–294. doi: 10.1016/S0376-7388(00)81316-2

Elferink, M. G. L., De Wit, J. G., Driessen, A. J. M., and Konings, W. N. (1994). Stability and proton-permeability of liposomes composed of archaeal tetraether lipids. *Biochim. Biophys. Acta* 1193, 247–254. doi: 10.1016/0005-2736(94)90160-0

Frolov, V. A., Shnyrova, A. V., and Zimmerberg, J. (2011). Lipid polymorphisms and membrane shape. *Cold Spring Harb. Perspect. Biol.* 3:a004747. doi: 10.1101/cshperspect.a004747

Gambacorta, A., Gliozzi, A., and De Rosa, M. (1995). Archaeal lipids and their biotechnological applications. *World J. Microbiol. Biotechnol.* 11, 115–131. doi: 10.1007/BF00339140

Gilmore, S. F., Yao, A. I., Tietel, Z., Kind, T., Facciotti, M. T., and Parikh, A. N. (2013). Role of squalene in the organization of monolayers derived

from lipid extracts of *Halobacterium salinarum*. *Langmuir* 29, 7922–7930. doi: 10.1021/la401412t

Gliozzi, A., Paoli Mario Rosa, G. D. E., and Gambacorta, A. (1983). Effect of isoprenoid cyclization on the transition temperature of lipids in thermophilic archaebacteria. *Biochem. Biophys. Acta* 735, 234–242. doi: 10.1016/0005-2736(83)90298-5

Goñi, F. M. (2014). The basic structure and dynamics of cell membranes: an update of the Singer-Nicolson model. *Biochim. Biophys. Acta Biomembr*. 1838, 1467–1476. doi: 10.1016/j.bbamem.2014.01.006

Hafenbradl, D., Keller, M., and Stetter, K. O. (1996). Lipid analysis of *Methanopyrus kandleri*. *FEMS Microbiol. Lett*. 136, 199–202. doi: 10.1111/j.1574-6968.1996.tb08049.x

Haines, T. H. (2001). Do sterols reduce proton and sodium leaks through lipid bilayers? *Prog. Lipid Res*. 40, 299–324. doi: 10.1016/S0163-7827(01)00009-1

Hauß, T., Dante, S., Dencher, N. A., and Haines, T. H. (2002). Squalane is in the midplane of the lipid bilayer: implications for its function as a proton permeability barrier. *Biochem. Biophys. Acta* 1556, 149–154. doi: 10.1016/S0005-2728(02)00346-8

Hauß, T., Dante, S., Haines, T. H., and Dencher, N. A. (2005). Localization of coenzyme Q10 in the center of a deuterated lipid membrane by neutron diffraction. *Biochim. Biophys. Acta Bioenerg*. 1710, 57–62. doi: 10.1016/j.bbabio.2005.08.007

Heberle, F. A., and Feigenson, G. W. (2011). Phase separation in lipid membranes. *Cold Spring Harb. Perspect. Biol*. 3, 1–13. doi: 10.1101/cshperspect.a004630

Heberle, F. A., Petruzi1'1elo, R. S., Pan, J., Drazba, P., Kučerka, N., Standaert, R. F., et al. (2013). Bilayer thickness mismatch controls domain size in model membranes. *J. Am. Chem. Soc*. 135, 6853–6859. doi: 10.1021/ja3113615

Jarsch, I. K., Daste, F., and Gallop, J. L. (2016). Membrane curvature in cell biology: an integration of molecular mechanisms. *J. Cell Biol*. 214, 375–387. doi: 10.1083/jcb.201604003

Jebbar, M., Franzetti, B., Girard, E., and Oger, P. (2015). Microbial diversity and adaptation to high hydrostatic pressure in deep-sea hydrothermal vents prokaryotes. *Extremophiles* 19, 721–740. doi: 10.1007/s00792-015-0760-3

Jouhet, J. (2013). Importance of the hexagonal lipid phase in biological membrane organization. *Front. Plant Sci.* 4:494. doi: 10.3389/fpls.2013.00494

Kates, M., and Manson, L. A. (1984). *Membrane Fluidity*. New York, NY: Plenum Press.

Katsaras, J. (1995). X-ray diffraction studies of oriented lipid bilayers. *Biochem. Cell Biol*. 73, 209–218. doi: 10.1139/o95-025

Langworthy, T. A., Tornabene, T. G., and Holzer, G. (1982). Lipids of Archaebacteria. *Zent. Bakteriol. Angew. Okol. Microbiol. Abt. L. Orig. C. Hyg*. 3, 228–244.

Marquardt, D., Heberle, F. A., Nickels, J. D., Pabst, G., and Katsaras, J. (2015). On scattered waves and lipid domains: detecting membrane rafts with X-rays and neutrons. *Soft Matter*. 11, 9055–9072. doi: 10.1039/C5SM01807B

Matsuno, Y., Sugai, A., Higashibata, H., Fukuda, W., Ueda, K., Uda, I., et al. (2009). Effect of growth temperature and growth phase on the lipid composition of the archaeal membrane from Thermococcus kodakaraensis. *Biosci. Biotechnol. Biochem*. 73, 104–108. doi: 10.1271/bbb.80520

McCarthy, N. L. C., Ces, O., Law, R. V., Seddon, J. M., and Brooks, N. J. (2015). Separation of liquid domains in model membranes induced with high hydrostatic pressure. *Chem. Commun*. 51, 8675–8678. doi: 10.1039/C5CC02134K

McMahon, H. T., and Boucrot, E. (2015). Membrane curvature at a glance. *J. Cell Sci*. 128, 1065–1070. doi: 10.1242/jcs.114454

Nagle, J. F., and Tristram-Nagle, S. (2000). Structure of lipid bilayers. *Biochim. Biophys. Acta* 1469, 159–195. doi: 10.1016/S0304-4157(00)00016-2

Oger, P. M., and Cario, A. (2013). Adaptation of the membrane in archaea. *Biophys. Chem*. 183, 42–56. doi: 10.1016/j.bpc.2013.06.020

Oger, P. M., and Jebbar, M. (2010). The many ways of coping with pressure. *Res. Microbiol*. 161, 799–809. doi: 10.1016/j.resmic.2010.09.017

Perutková, Š., Daniel, M., Dolinar, G., Rappolt, M., Kralj-Iglič, V., and Iglič, A. (2009). Stability of the inverted hexagonal phase, *Adv. Planar Lipid Bilayers Liposomes*, 9, 237–278. doi: 10.1016/S1554-4516(09)09009-7

Peters, J., Golub, M., Demé, B., Gonthier, J., Maurice, J., Payre, C., et al. (2018). New pressure cells for membrane layers and systems in solutions up to 100°C. *J. Neutron Res*. 20, 1–10. doi: 10.3233/JNR-180055

Richard, D., Ferrand, M., and Kearley, G. J. (1996). Analysis and visualisation of neutron-scattering data. *J. Neutron Res*. 4, 33–39. doi: 10.1080/10238169608200065

Sako, Y., Nomura, N., Uchida, A., Ishida, Y., Morii, H., Koga, Y., et al. (1996). *Aeropyrum pernix* gen. nov., sp. nov., a novel aerobic hyperthermophilic archaeon growing at temperatures up to 100°C. *Int. J. Syst. Bacteriol*. 46, 1070–1077. doi: 10.1099/00207713-46-4-1070

Salvador-Castell, M., Brooks, N. J., Peters, J., and Oger, P. (2020a). Induction of non-lamellar phases in archaeal lipids at high temperature and high hydrostatic pressure by apolar polyisoprenoids. *Biochim. Biophys. Acta Biomembr*. 1862:183130. doi: 10.1016/j.bbamem.2019.183130

Salvador-Castell, M., Déme, B., Misuraca, L., Oger, P., and Peters, J. (2019). *Novel High-Pressure/High-Temperature Phases in Archaeal Membranes*. Institut Laue-Langevin (ILL). doi: 10.5291/ILL-DATA.8-02-852

Salvador-Castell, M., Demé, B., Oger, P., and Peters, J. (2020b). Lipid phase separation induced by the apolar polyisoprenoid squalane demonstrates its role in membrane domain formation in archaeal membranes. *Langmuir* 36, 7375–7382. doi: 10.1021/acs.langmuir.0c00901

Salvador-Castell, M., Demé, B., Oger, P., and Peters, J. (2020c). Structural characterization of an archaeal lipid bilayer as a function of hydration and temperature. *Int. J. Mol. Sci*. 21:1816. doi: 10.3390/ijms21051816

Schmid, F. (2017). Physical mechanisms of micro- and nanodomain formation in multicomponent lipid membranes. *Biochim. Biophys. Acta* 1859, 509–528. doi: 10.1016/j.bbamem.2016.10.021

Schouten, S., Van Der Meer, M. T. J., Hopmans, E. C., Rijpstra, W. I. C., Reysenbach, A. L., Ward, D. M., et al. (2007). Archaeal and bacterial glycerol dialkyl glycerol tetraether lipids in hot springs of Yellowstone National Park. *Appl. Environ. Microbiol*. 73, 6181–6191. doi: 10.1128/AEM.00630-07

Shearman, G. C., Ces, O., Templer, R. H., and Seddon, J. M. (2006). Inverse lyotropic phases of lipids and membrane curvature. *J. Phys. Condens. Matter* 18:S1105–24. doi: 10.1088/0953-8984/18/28/S01

Siliakus, M. F., van der Oost, J., and Kengen, S. W. M. (2017). Adaptations of archaeal and bacterial membranes to variations in temperature, pH and pressure. *Extremophiles* 21, 651–670. doi: 10.1007/s00792-017-0939-x

Sinensky, M. (1974). Homeoviscous adaptation: a homeostatic process that regulates the viscosity of membrane lipids in *Escherichia coli*. *Proc. Natl. Acad. Sci. U.S.A*. 71, 522–525. doi: 10.1073/pnas.71.2.522

Singer, S. J., and Nicolson, G. L. (1972). The fluid mosaic model of the structure of cell membranes. *Science* 175, 720–731. doi: 10.1126/science.175.4023.720

Sprott, G. D., Agnew, B. J., and Patel, G. B. (1997). Structural features of ether lipids in the archaeobacterial thermophiles pyrococcus furiosus, *Methanopyrus kandleri*, *Methanothermus fervidus*, and *Sulfolobus acidocaldarius*. *Can. J. Microbiol*. 43, 467–476. doi: 10.1139/m97-066

Takai, K., Nakamura, K., Toki, T., Tsunogai, U., Miyazaki, M., Miyazaki, J., et al. (2008). Cell proliferation at 122°C and isotopically heavy CH4 production by a hyperthermophilic methanogen under high-pressure cultivation. *Proc. Natl. Acad. Sci. U.S.A*. 105, 10949–10954. doi: 10.1073/pnas.0712334105

Tayebi, L., Ma, Y., Vashaee, D., Chen, G., Sinha, S. K., and Parikh, A. N. (2012). Long-range interlayer alignment of intralayer domains in stacked lipid bilayers. *Nat. Mater*. 11, 1074–1080. doi: 10.1038/nmat3451

Tornabene, T. G., and Langworthy, T. A. (1979). Diphytanyl and dibiphytanyl glycerol ether lipids of methanogenic archaebacteria. *Science* 203, 51–53. doi: 10.1126/science.758677

Trapp, M., Marion, J., Tehei, M., Demé, B., Gutberlet, T., and Peters, J. (2013). High hydrostatic pressure effects investigated by neutron scattering on lipid multilamellar vesicles. *Phys. Chem. Chem. Phys*. 15, 20951–20956. doi: 10.1039/c3cp52762j

Tristram-Nagle, S. A. (2007). Preparation of oriented, fully hydrated lipid samples for structure determination using X-ray scattering. *Methods Mol. Biol*. 400, 63–75. doi: 10.1007/978-1-59745-519-0_5

Trovaslet-Leroy, M., Martinez, N., Marion, J., and Peters, J. (2016). "Hautes pressions et dynamique des systems bilogiques," in *Mesures en Conditions Extrêmes*, eds Y. Le Godec, H. Cardon, T. Hammouda, and Y. Morizet (Paris: Éditions des Archives Contemporaines), 51–64.

Tyler, A. I. I., Law, R. V., and Seddon, J. M. (2015). "X-Ray diffraction of lipid model membranes," in *Methods in Membrane Lipids*, ed D. M. Owen (New York, NY: Humana Press), 199–225.

Winter, R., and Jeworrek, C. (2009). Effect of pressure on membranes. *Soft Matter*. 5, 3157–3173. doi: 10.1039/b901690b

Yamauchi, K., Doi, K., Yoshida, Y., and Kinoshita, M. (1993). Archaebacterial lipids: highly proton-impermeable membranes from 1,2-diphytanyl-sn-glycero-3-phosphocholine. *Biochim. Biophys. Acta* 1146, 178–182. doi: 10.1016/0005-2736(93)90353-2

Yayanos, A. A., Dietz, A. S., and Van Boxtel, R. (1981). Obligately barophilic bacterium from the mariana trench. *Proc. Natl. Acad. Sci. U.S.A.* 78, 5212–5215. doi: 10.1073/pnas.78.8.5212

Zeng, X., Birrien, J. L., Fouquet, Y., Cherkashov, G., Jebbar, M., Querellou, J., et al. (2009). Pyrococcus CH1, an obligate piezophilic hyperthermophile: extending the upper pressure-temperature limits for life. *ISME J.* 3, 873–876. doi: 10.1038/ismej.2009.21

Conflict of Interest: The authors declare that the research was conducted in the absence of any commercial or financial relationships that could be construed as a potential conflict of interest.

Copyright © 2020 LoRicco, Salvador-Castell, Demé, Peters and Oger. This is an open-access article distributed under the terms of the Creative Commons Attribution License (CC BY). The use, distribution or reproduction in other forums is permitted, provided the original author(s) and the copyright owner(s) are credited and that the original publication in this journal is cited, in accordance with accepted academic practice. No use, distribution or reproduction is permitted which does not comply with these terms.